Effect of Patient Motion on Tomographic Myocardial Perfusion Imaging

Jeffrey A. Cooper, Paul H. Neumann, and Brian K. McCandless

Department of Radiology, Albany Medical College, Albany, New York

We evaluated the effect of patient motion on inducing false-positive tomographic ^{201}Tl myocardial perfusion studies. The effects of the angle of camera rotation at which movement occurs, the direction of movement and the distance of movement were studied. Movement was simulated by shifting the raw data from normal motion-free ^{201}Tl tomographic myocardial perfusion studies. The visual detectability of motion artifact was evaluated with receiver-operating characteristic curve analysis. The clinical importance of patient movement was determined by measuring the incidence of quantitative bull's-eye abnormalities induced by motion. Visual artifacts were more detectable and quantitative abnormalities more frequent as the distance of movement increased. Artifacts from 3.25 mm of movement were not visually detectable. Artifacts from 6.5 mm of movement were visually detectable, but were infrequently clinically important. Movement of 13 mm or greater frequently caused quantitative abnormalities. Quantitative abnormalities from axial movement were more frequent than artifacts from lateral movement. Quantitative abnormalities were more frequent when the movement occurred at the beginning or end. We conclude that when patients move during ^{201}Tl tomographic myocardial perfusion imaging, the incidence and character of false-positive results depend on the angle of camera rotation at which the movement occurs, the direction of the movement and distance of the movement.

J Nucl Med 1992; 33:1566–1571

Myocardial perfusion imaging plays an increasingly important role in the management of coronary artery disease (CAD) (*1,2*). Single-photon emission computed tomography (SPECT) can increase the sensitivity, specificity and anatomic localization of myocardial perfusion imaging for CAD (*3,4*). However, optimal SPECT imaging requires strict attention to quality control and recognition of imaging artifacts (*5*).

Patient motion commonly degrades SPECT myocardial imaging (*5,6*). Patients often have difficulty in hyperextending their left arm and remaining still 20–30 min due to arthritis, weakness and postexercise fatigue. When patients move during image acquisition, the resultant artifacts may be confused with ischemia by both visual (*5,7*) and quantitative (*7*) criteria. Optimal SPECT myocardial imaging requires recognition of clinically important motion artifacts.

Multiple types and degrees of patient movement can occur during a SPECT study. The patient may abruptly move along the axis of rotation or lateral to the imaging table. Movement can occur at various times during the camera rotation arc. The distance of movement may vary as well. The type and degree of patient movement may influence the presence and clinical importance of the resultant motion artifacts (*8*).

There is a limited understanding of how patient movement interferes with the diagnosis of CAD (*7,8*). Some investigators have described motion artifacts with as little as 3.25 mm of movement at the midpoint of a thallium acquisition (*7*). Others have found that thallium myocardial imaging studies are tolerant to up to 6.5–13 mm of patient movement (*8*). Others have presented anecdotal cases of patient movement resulting in image artifacts (*5, 6,10*). However, the effects of motion on thallium myocardial perfusion imaging have not been systematically evaluated.

The purpose of this investigation was to determine the relationship between the distance of movement, the direction of movement and the camera angle at which movement occurs to the presence of motion artifact. The detectability of motion artifact in reconstructed images was determined by receiver-operating characteristic (ROC) curve analysis of blinded visual readings. The clinical significance of motion artifact was determined by interpreting images with quantitative bull's-eye analysis using standardized criteria for abnormality (*2*).

MATERIALS AND METHODS

The data base consisted of normal motion-free postexercise ^{201}Tl SPECT studies performed on patients referred for evaluation of myocardial perfusion. Patients underwent treadmill exercise stress tests and were injected with 3 mCi of ^{201}Tl-chloride. The images were acquired on a General Electric 400AC gamma camera with a high-resolution, low-energy collimator and consisted of 32 40-sec 64 × 64 images over a 180° arc from the 45°

Received Nov. 14, 1991; revision accepted Mar. 10, 1992.
For reprints contact: Jeffrey A. Cooper, MD, Nuclear Medicine, A-72, 47 Scotland Ave, Albany Medical Center, Albany, NY 12208.

right anterior oblique (RAO) to the 45° left posterior oblique (LPO). Only poststress images were used. Studies had to be both motion-free and normal to be included. Studies were considered motion-free if there was less than 3.25 mm (0.5 pixels) of movement by the cross-correlation method (*9*), no detectable movement on both visual inspection of a rotating cinegraphic display and on summed images and no streaking or smudging on reconstructed images. Studies were considered normal if they appeared normal by visual analysis and were quantitatively normal by bull's-eye analysis (*1*).

Movement was simulated by shifting the planar images. Axial movement (along the length of the exam table) was simulated by shifting the images vertically. Lateral movement (along the width of the exam table) was simulated by shifting the images horizontally according to the formula:

$$d_i = d_T \cdot \cos(\phi_i),$$

where d_i is the horizontal distance to shift image i, d_T is the distance of patient movement being simulated and ϕ_i is the angle of the camera to the patient for image i with 0° corresponding to the anterior image. The shifting was divided proportionately between the images before and after the point of movement to minimize translation of the reconstructed image. For example, 6.5 mm of upward movement at 22.5° (the eighth image) was obtained by shifting the first eight images down 4.5 mm and the last 24 images up 1.5 mm.

The planar images were filtered with a two-dimensional Metz filter (*11*) optimized for the camera used for acquisition (*12*) and then backprojected with a ramp filter to produce transaxial slices. The transaxial images were reconstructed along the short, horizontal long and vertical long axes. The transaxial resolution of the reconstructed images was 11 mm (FWHM) for a point source in air.

To determine the amount of movement that can cause a visually detectable motion artifact, we measured the accuracy with which an observer could distinguish between motion artifact and variations in reconstruction. An observer was shown a pair of reconstructed thallium images. The first image set was reconstructed from motion-free images. The second image set consisted of the same image set randomized blindly to contain or not contain movement with a 50% probability, and then reconstructed using angles and limits determined independently from those used for the first image set. If the second image set was randomized to not contain movement, all 32 images were shifted 3.25 mm (0.5 pixels) to control for smoothing of the simulated motion image sets caused by nonintegral shifts. The observer viewed both data sets simultaneously on a 256 gray scale monochrome monitor and knew which data set was the motion-free data set and which data set possibly contained motion. The second image set was scored on a five-point scale according to the certainty that it contained motion (1: definitely no motion artifact, 2: probably no motion artifact, 3: uncertain, 4: probable motion artifact, 5: definite motion artifact). For each trial the distance, direction and camera angle at the time of movement were constant. Training trials (n = 40) and then testing trials (n = 60) were conducted for all combinations of 3.25, 6.5, 13 and 19.5 mm of movement (0.5, 1.0, 2.0 and 3.0 pixels, respectively) in the axial and lateral directions occurring at camera angles of −22.5°, 0°, 22.5°, 45°, 67.5°, 90°, and 112.5° (corresponding to frame numbers 4, 8, 12, 16, 20, 24 and 28 respectively). Different patients were used for the training sets and testing trials.

The diagnostic accuracy of the visual detection of motion artifact was determined by ROC curve analysis using the computer program ROCFIT (*13,14*). The area under the ROC curve (z score or A_z) was interpreted as the accuracy for detecting motion artifact when the prevalence of patient movement was 50% (*13*). An accuracy significantly greater than 50% at the 0.05 probability level by Student's t-test was considered to indicate detectable motion artifact.

To determine the amount of motion that can cause a quantitative abnormality, we performed bull's-eye analysis studies with simulated movement (*2,15*). The bull's-eyes from studies with simulated movement were compared to a normal data base. The normal data base consisted of the average of the bull's-eyes from the control group of motion-free studies. The same reconstruction angles and limits used to make the normal data base were used for the images with simulated motion. A pixel was considered to be abnormal if it was more than 2.5 s.d.s below the mean of the corresponding pixel in the normal data base (*2,15*). The criteria for abnormality in a stress bull's-eye image was 12% abnormal pixels in the left anterior descending coronary artery territory, 12% abnormal pixels in the circumflex coronary artery territory, or 8% abnormal pixels in the right coronary artery territory (*2, 15*). For each trial the distance, direction and camera angle at the time of movement were constant. Trials (n = 60) were conducted for all combinations of 3.25, 6.5, 13 and 19.5 mm of movement in the axial and lateral directions occurring at camera angles of −22.5°, 0°, 22.5°, 45°, 67.5°, 90° and 112.5°.

The incidence of bull's-eye abnormalities were tabulated and standard deviations and 95% confidence limits were calculated (*16*). An incidence greater than 5% was defined as being clinically important. The significance of differences in distributions were determined by chi-square.

RESULTS

Figure 1 shows a set of representative ROC curves and their corresponding accuracies (z score or A_z) for the visual detectability of axial motion of 3.25, 6.5 and 13 mm occurring at the 45° camera angle (left anterior oblique projection). Figure 2 shows the accuracy of visually detecting motion artifact as a function of the distance, direc-

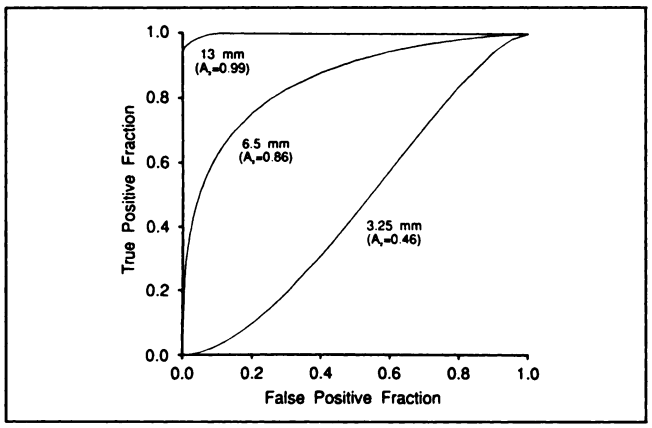

FIGURE 1. Representative ROC curves and their corresponding accuracies (A_z) for the visual detectability of axial motion of 3.25, 6.5 and 13 mm occurring at the 45° camera angle (LAO projection).

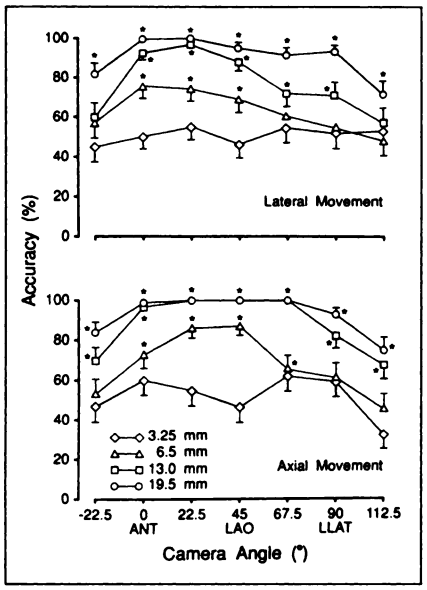

FIGURE 2. Visual detectability of motion artifact. Values shown are the accuracy of visually detectingmotion artifact ± s.e.m. (determined by ROC curve analysis) as a function of camera angle, distance of motion and direction of motion. *p < 0.05 different from 50%; ANT = anterior projection; LAO = left anterior oblique projection; and LLAT = left lateral projection.

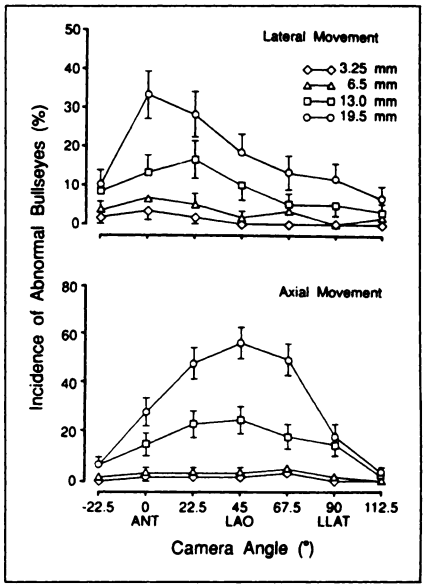

FIGURE 3. Effect of patient movement on quantitative bull's-eye analysis. Values shown are the incidence ± s.d. of abnormal bull's-eyes as a function of the distance, direction and camera angle of motion. ANT = anterior projection; LAO = left anterior oblique projection; and LLAT = left lateral projection.

tion and timing of movement. The timing of movement is referred to by the camera angle at which motion occurs. Values shown are mean ± s.e.m. accuracy as determined by ROC curve analysis. An accuracy of 50% is achievable by random selection and therefore indicates no detectability of an artifact (*13*). Values that are starred are different from 50% ($p < 0.05$). Movement of 3.25 mm did not cause a detectable artifact. Movement of 6.5 mm caused a detectable artifact when the motion occurred between the anterior and left lateral projections ($p < 0.05$). In general, movement of greater than 13 mm always caused a detectable artifact. Motion artifact was more detectable with greater distances of movement ($p < 0.05$) and when the movement occurred at the midpoint of camera rotation as compared to the ends of camera rotation ($p < 0.05$). At distances greater than 3.25 mm, motion artifact from axial movement was more detectable than motion artifact from lateral movement ($p < 0.05$).

Figure 3 shows the incidence of abnormal bull's-eye analyses as a function of the distance, direction and timing of movement. The data shown are the mean ± standard deviation incidence of abnormality. A bull's-eye with more than one abnormal vascular territory was counted as a single abnormality. The incidence of abnormal bull's-eyes with 3.25 mm of axial movement 1.2% (95% confidence interval 0.4%–2.9%), for 3.25 mm of lateral movement was 1.0% (95% confidence interval 0.3%–2.6%), for 6.5 mm of axial movement 2.6% (95% confidence interval 1.4%–4.8%) and for 6.5 mm of lateral movement 3.1% (95% confidence interval 1.7%–5.4%). The incidence with lateral movement of 6.5 mm was greater than 5% when the motion occurred between the anterior and left lateral projections. In general, movement of greater than 13 mm resulted in an incidence of abnormal bull's-eyes of greater than 5%. Abnormal bull's-eyes were more frequent with greater distances of movement ($p < 0.05$). For axial movement, abnormal bull's-eyes were more frequent when the movement occurred at the midpoint of camera rotation as compared to the ends of camera rotation ($p < 0.05$). For lateral movement, abnormal bull's-eyes were more frequent when the movement occurred during the anterior projection (0°) as compared to the ends of camera rotation ($p < 0.05$). At distances greater than 6.5 mm, axial movement resulted in a greater incidence of abnormal bull's-eyes than lateral movement ($p < 0.05$).

Figure 4 shows the incidence of quantitative bull's-eye abnormalities with 19.5 mm of movement by vascular territory as a function of the direction and timing of

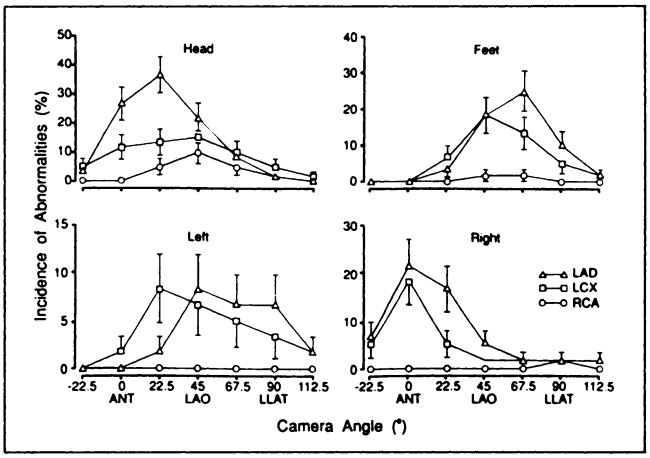

FIGURE 4. Effect of 19.5 mm of patient movement on quantitative bull's-eye analysis by vascular territory. Values shown are the incidence ± s.d. of abnormal bull's-eyes as a function of the direction of motion and the camera angle at which motion occurred. Head, feet, left and right refer to motion of the patient directed towards their head, feet, left side and right side, respectively. LAD = left anterior descending coronary artery territory; LCX = circumflex coronary artery territory; RCA = right coronary artery territory; ANT = anterior projection; LAO = left anterior oblique projection; and LLAT = left lateral projection.

movement. The data shown are the mean ± standard deviation incidence of abnormalities. Head, feet, left and right refer to movement directed towards the patient's head, feet, left side and right side, respectively. In general, the left anterior descending coronary artery territory was most susceptible to motion artifact and the right coronary artery territory was the least susceptible. The distribution of abnormalities among camera angles differed according to the direction of motion ($p < 0.05$).

DISCUSSION

We evaluated the effect that patient movement has on inducing false-positive ^{201}Tl tomographic myocardial perfusion studies. Patient movement caused visually detectable artifacts in a manner that depended on the camera angle at which the movement occurred, the direction of the movement and the distance of the movement (Fig. 2). Patient movement also caused quantitative bull's-eye abnormalities in a manner that depends on the timing, direction and the distance of movement (Fig. 3).

For the ROC investigation of the visual detectability of motion artifact, the observer was provided the control motion-free study for comparison. This procedure maximized the detectability of motion artifact by allowing the observer to find subtle differences between the experimental and control images which otherwise might not be recognizable. The procedures of randomization and blinded reading required that the reader differentiate motion artifact from minor differences in reconstruction. Thus, if movement is not visually detectable under the circumstances of this ROC study, it is unlikely to be clinically important.

Visual detection of an artifact is not the same as visual detection of a clinically abnormal pattern of thallium uptake, that is, one that might be confused with infarction or ischemia. The data in Figure 2 shows the reader's ability to detect any difference between the control and experimental images regardless of whether the artifact was considered a clinically important abnormality. To define whether this difference could be confused with ischemia or infarction is difficult because of the subjective criteria used to make this diagnosis. To address the clinical relevance of motion, we analyzed the data using the quantitative criteria for CAD that have been adopted in bull's-eye analysis (*2,15*). Motion that resulted in a quantitative abnormality by standard criteria was categorized as being clinically significant.

To maximize the quantitative detection of abnormalities, we used the study group as its own control, rather than using the commercially supplied normal data base. This allowed us to control the reconstruction methods used for creating the normal data base. Our data base was not designed to diagnose CAD, but to predict the incidence and location of false-positives produced by motion when using standard methods of quantitative analysis (*2,15*).

By quantitative bull's-eye analysis, patient movement caused abnormalities in a manner which depended on the direction of the movement, the camera angle at which the movement occurred, and the distance of the movement (Fig. 3). When compared to the data in Figure 2, the accuracy of detecting motion artifacts is generally higher than the incidence of abnormalities. This indicates that motion may produce visually detectable artifacts which are not clinically important. For some types of movement (such as 6.5 mm of axial movement), motion artifacts were frequently detectable, but were infrequently the cause of a quantitative abnormality.

The effect of patient movement depended highly on the distance of the motion (Figs. 2 and 3). Visual artifacts with 3.25 mm of movement were not detectable and the incidence of quantitative abnormalities with movement of 3.25 mm was less 2.9% and 2.6% for the axial and lateral directions, respectively (Fig. 2). Greater distances of movement caused visually detectable artifacts (Fig. 2), although 6.5 mm of movement resulted in an incidence of quantitative abnormalities less than 4.8% and 5.4% for the axial and lateral directions, respectively (Fig. 3). These findings indicate that motion of less than 6.5 mm is unlikely to cause clinically important abnormalities in a normal study, although motion between 3.25 and 6.5 mm may cause visually detectable changes in the quality of a thallium study. The results suggest that abnormalities consistent with infarction or ischemia in a thallium myocardial perfusion study have a low likelihood of being caused by a motion artifact, if the distance of motion is less than 6.5 mm.

The reasons why tomographic imaging of myocardial perfusion tolerate up to 6.5 mm of movement are unknown. One explanation may be related to the resolution of the camera. In this study, motion did not induce frequent artifacts until the degree of motion was on the order of the camera resolution. Although the camera resolution in air was 11 mm, the actual resolution during myocardial perfusion imaging was likely larger due to tissue scatter and attenuation. Myocardial perfusion studies obtained on cameras with system resolutions better than the camera used in this study may be less tolerant to patient motion.

Another explanation for the observed tolerance to small distances of motion may be related to the fact that thallium tomographic myocardial perfusion imaging is confounded by motion of the heart from its contraction and its respiratory excursion as it sits on the diaphragm. Observation of R-wave gated blood-pool studies of the heart or respiratory gated perfusion lung scans demonstrated more than 19.5 mm of movement (*17*). Despite the magnitudes of the movements of the heart and lungs, SPECT imaging artifacts due to cardiac and resting respiratory motion have not been described. The tolerance of SPECT imaging to respiratory and cardiac motion may be related to the low-pass filter in backprojection methods which may blur small degrees of movement. The factors that make SPECT imaging tolerant to cardiac and respiratory motion may

also make SPECT imaging tolerant to patient movement of similar magnitudes.

The effect of patient movement depended on the camera angle during which the motion occurred (Figs. 2 and 3). Motion which occurred at the beginning or end of the camera rotation was less likely to cause a detectable artifact or a quantitative abnormality than motion in the middle of the arc (Figs. 2 and 3). As motion occurs earlier or later in the study, a larger percentage of the raw images are projections of a single unmoved distribution of radioactivity. As motion occurs towards the middle of the study, the images become more evenly split between projections of two different distributions of radioactivity, one before the movement and one after the movement. With lateral motion, the situation becomes more complicated as the effect of the motion is greatest in the anterior image (when the motion is parallel to the camera) and least in the lateral projection (when the motion is perpendicular to the camera). Therefore with lateral motion, there is a skew of the greatest effect of motion towards anterior camera projections (Fig. 3).

The effect of patient movement also depended on the direction of motion (Figs. 2 and 3). Axial movement was more detectable and caused a higher incidence of abnormalities than lateral movement. The projected distance of axial movement is always greater than the same distance of lateral movement, except in the anterior image (when the camera is parallel to the direction of motion). Thus, it can be expected that axial movement will have a greater effect than lateral movement. The affected vascular territory depended on whether the patient moved in the direction of their head, feet, left side or right side (Fig. 4).

This analysis examined the effect of movement on normal poststress thallium studies and the tolerance of normal thallium studies to visually detectable motion artifact nor quantitative abnormalities. It is unknown whether these data will apply to the induction of normal patterns when there are defects in myocardial perfusion. Furthermore, the tolerance of abnormal myocardial perfusion patterns to motion may be different than that of normal myocardial perfusion patterns.

Other types of movement can occur which were not evaluated in this study. Patients may rotate on the plane of the examining table or may rotate about the axis of camera rotation. All patients have some physiologic respiratory and cardiac motion and the respiratory movement may vary during the course of a study and give rise to upward creep, a common source of motion artifact (*18*). In addition, there may be combinations of translation and rotation or complex motion which cannot be expressed in terms of translation and rotation. The effect of these types of motion on ^{201}Tl myocardial tomographic imaging was not evaluated.

The current findings are discordant with those reported by Eisner and others (*7*). They examined the effect of simulated nonreturning axial movement of various distances on 10 normal thallium studies. In contrast to the current data, they found that 3.25 and 6.5 mm axial movement resulted in 15% and 40% false-positive rates, respectively. This discrepancy may be explained by several differences in methodology. In the study of Eisner et al., visual examination of images were not blinded and the criteria used to determine an abnormality were not specified. Second, only axial movement at the midpoint of camera rotation was examined, which our data indicated to be the most sensitive to induction of motion artifact (Figs. 2 and 3). Third, the reconstruction and quantitative analysis methods were different. The tolerance of tomographic imaging to patient motion may be dependent on image acquisition and processing methods. With our methods, we found that 3.25 mm of axial movement was not detectable by a blinded observer (Fig. 2) and that although 6.5 mm of axial movement was readily detectable by a blinded observer (Fig. 2), it caused a low frequency of abnormalities according to our quantitative criteria (Figs. 3 and 4).

Several investigators have reported automated methods for detecting patient movement and correcting for the effects of patient movement (*7,9,10*). The results of the current study imply that less than 6.5 mm of movement does not need to be detected or corrected. It may be important not to apply motion correction needlessly since some motion correction programs may occasionally degrade image quality (*10*).

There is much interest in the use of ^{99m}Tc agents for myocardial perfusion imaging. Our results suggest that motion will cause artifacts in ^{99m}Tc myocardial perfusion images in a manner that depends on the camera angle at which the movement occurs and the distance and direction of movement. However, image resolution may vary among the myocardial perfusion agents because of factors such as count density and different optimal filters. This may cause the incidence of abnormalities at a given direction, distance and camera angle to differ among myocardial perfusion agents. Also, because of variations in organ distribution among the myocardial perfusion agents, such as greater liver uptake in the ^{99m}Tc based perfusion agents, the type of artifacts produced may differ as well.

CONCLUSION

In summary, we evaluated the effect of patient movement on inducing false-positive ^{201}Tl tomographic myocardial perfusion studies. The effect of patient movement depends on the camera angle at which the movement occurs, the direction of the movement and distance of the movement. Patient movement at very beginning or end of a study is less likely to result in image artifacts than movement in the middle of an acquisition. The effect of patient movement in the axial direction is greater than the effect of movement in the lateral direction. Patient movement of 3.25 mm or less does not result in detectable imaging artifacts. Movement of between 3.25 and 6.5 mm

may be clinically detectable, but is unlikely to cause quantitatively important image artifacts. Movement of greater than 6.5 mm can cause clinically important image artifacts and must be considered as a potential source of error in ^{201}Tl tomographic myocardial perfusion studies.

REFERENCES

1. Garcia EV, DePuey EG, Sonnemaker RE, et al. Quantification of the reversibility of stress-induced thallium-201 myocardial perfusion defects: a multicenter trial using bull's-eye polar maps and standard normal limits. *J Nucl Med* 1990;31:1761–1765.
2. Van Train KF, Maddahi J, Berman DS, et al. Quantitative analysis of tomographic stress thallium-201 myocardial scintigrams: a multicenter trial. *J Nucl Med.* 1990;31:1168–1179.
3. Ritchie JL, Williams DL, Harp G, Stratton JL, Caldwell JH. Transaxial tomography with thallium-201 for detecting remote myocardial infarction. Comparison with planar imaging. *Am J Cardiol* 1982;50:1236–1241.
4. Fintel DJ, Links JM, Brinker JA, Frank TL, Parker M, Becker LC. Improved diagnostic performance of exercise thallium-201 single photon emission computed tomography over planar imaging in the diagnosis of coronary artery disease: a receiver operating characteristic analysis. *J Am Coll Cardiol* 1989;13:600–612.
5. DePuey EG, Garcia EV. Optimal specificity of thallium-201 SPECT through recognition of imaging artifacts. *J Nucl Med* 1989;30:441–449.
6. Friedman J, Berman DS, Van Train K, et al. Patient motion in thallium-201 myocardial SPECT imaging: an easily identified frequent source of artifactual defect. *Clin Nucl Med* 1988;13:321–324.
7. Eisner R, Churchwell A, Noever T, et al. Quantitative analysis of the tomographic thallium-201 myocardial bull's-eye display: Critical role of correcting for patient motion. *J Nucl Med* 1988;29:91–97.
8. Zhu YY, Botvinick EH, O'Connell WJ, Dae MW. Tolerance of SPECT perfusion imaging to patient motion [Abstract]. *J Nucl Med* 1990;31:841.
9. Eisner RL, Noever T, Nowak D, et al. Use of cross-correlation function to detect patient motion during SPECT imaging. *J Nucl Med* 1987;28: 97–101.
10. Geckle WJ, Frank TL, Links JM, Becker LC. Correction for patient motion and organ movement in SPECT: application to exercise thallium-201 cardiac imaging. *J Nucl Med* 1988;29:441–450.
11. King MA, Doherty PW, Schwinger RB, Jacobs DA, Kidder RE, Miller TR. Fast count-dependent digital filtering of nuclear medicine images: concise communication. *J Nucl Med* 1983;24:1039–1045.
12. Gilland DR, Tsui BMW, McCartney WH, Perry JR, Berg J. Determination of the optimum filter function for SPECT imaging. *J Nucl Med* 1988;29: 643–650.
13. Hanley JA, McNeil BJ. The meaning and use of the area under a receiver operating characteristic (ROC) curve. *Radiology* 1982;143:29–36.
14. Metz CE. ROC Methodology in radiologic imaging. *Invest Radiol* 1986; 21:720–733.
15. Maddahi J, Van Train K, Prigent F, et al. Quantitative single photon emission computed tomography for detection and localization of coronary artery disease: optimization and prospective validation of a new technique. *J Am Coll Cardiol* 1989;14:1689–1699.
16. Diamond GA. Limited assurances. *Am J Cardiol* 1989;63:99–100.
17. Line BR, Cooper JA, Spicer KE, Jones AE, Crystal RG, Johnson GS. Radionuclide cinepneumography: flow-volume imaging of the respiratory cycle. *J Nucl Med* 1980;21:219–224.
18. Friedman J, Van Train K, Maddahi J, et al. "Upward creep" of the heart: a frequent source of false-positive reversible defects during thallium-201 stress-redistribution SPECT. *J Nucl Med* 1989;30:1718–1722.

EDITORIAL

Sensitivity of SPECT Thallium-201 Myocardial Perfusion Imaging to Patient Motion

In this month's issue, Cooper et al. have simulated both vertical and horizontal patient motion during SPECT ^{201}Tl myocardial perfusion imaging and they determined the relationship between the amount and timing (frame at which motion occurred) of patient motion and false-positive SPECT ^{201}Tl images (*1*). As our group had done, studies were read normal or abnormal based on quantitative criteria applied to bull's-eye analysis. In comparison to our findings, the results of Cooper et al. show a markedly decreased sensitivity to patient motion. Table 1 summarizes the disparate results on the frequency of false-positive findings for patient scans with simulated motion, which occurred half-way through the SPECT scan.

Previously, our group described a technique which detects and corrects for vertical (i.e., head-to-foot) patient motion during SPECT ^{201}Tl myocardial perfusion imaging (*2,3*). We also evaluated the sensitivity of SPECT ^{201}Tl to patient motion by quantitative bull's-eye analysis of (low probability of disease) patient data sets with *simulated* patient motion (*2*). Motion was simulated by "moving" the SPECT view data from ± 0.5 to ± 3.0 pixels for views 17–32 of a 32 view/180° SPECT acquisition. The SPECT data then were reconstructed, and reformatted into short-axis slices. The short-axis slices were processed through our own version of the bull's-eye program [REV 3.0 on the General Electric STAR system, and later used on other General Electric computer systems (*4*)] using a gender-matched normal file consisting of 50 females and 50 males (*5*). Each simulated data set was processed as an independent study so that slice selection, angle se-

TABLE 1
Comparison of False-Positive Findings for Motion That Occurred in the Middle of the SPECT Scan

Degree of motion (mm)	Eisner et al. (2)	Cooper et al. (1)
3.25	15%	2.9%
6.5	40%	4.8%
13	80%	20%
26	80%	55%

Received Apr. 14, 1992; accepted Apr. 15, 1992.

For reprints contact: Robert L. Eisner, PhD, Carlyle Fraser Heart Center, Crawford Long Hospital of Emory University, Department of Nuclear Cardiology, 550 Peachtree St., Atlanta, GA 30365.